Korean J. Chem. Eng., 32(8), 1522-1527 (2015)
DOI: 10.1007/s11814-014-0359-x

pISSN: 0256-1115
eISSN: 1975-7220

Hydrogen selectivity and permeance effect on the water gas shift reaction (WGSR) in a membrane reactor

Hankwon Lim†

Department of Chemical Systematic Engineering, Catholic University of Daegu,
13-13, Hayang-ro, Hayang-yep, Gyeongsan, Gyeongbuk 712-702, Korea
(*Received 22 May 2014 • accepted 2 December 2014*)

Abstract−Simulated results are presented using a reaction rate equation and a one-dimensional reactor model for a water gas shift reaction (WGSR) in a membrane reactor (MR) with a feed stream obtained from coal gasifiers. CO conversion in a MR at 423-573 K was higher than equilibrium conversion at the same temperature. The effect of two important parameters of a membrane, hydrogen selectivity and hydrogen permeance, on MR performance was studied and hydrogen selectivity was favorable for enhanced CO conversion, reduced CO concentration, and enhanced fuel-cell grade hydrogen. Hydrogen permeance was also favorable for CO conversion enhancement in a MR due to an increased driving force between the shell side (retentate) and the tube side (permeate) of a membrane. The criteria of a hydrogen permeance of higher than 8×10^{-8} mol $m^{-2}s^{-1}Pa^{-1}$ and a hydrogen selectivity of 100 were suggested to produce a fuel-cell grade hydrogen (CO concentration less than 50 ppm) in the permeate and a concentrated CO_2 (more than 90%) in the retentate simultaneously in a MR.

Keywords: Water Gas Shift Reaction (WGSR), Membrane Reactor (MR), Hydrogen Selectivity, Hydrogen Permeance, Numerical Simulation

INTRODUCTION

Recently, there has been a strong demand for hydrogen in many industrial sectors such as petroleum, petrochemical, and fuel-cell. Currently, most of hydrogen used in the world is commercially produced by catalytic reforming of methane using Ni-based catalysts in a steam reformer. Much attention has been paid to the concept of a membrane reactor (MR) to produce enhanced hydrogen as means to meet the high demand for hydrogen. Fig. 1 shows the comparison between a conventional reactor/separator and a MR. A MR can be employed in various industrial applications for a compact design and cost savings by combining two units (reactor and separator) into one single unit (MR). Furthermore, improved reactant conversion and product yield can be achieved by continuously removing one of products of interest through a membrane [1]. For example, higher conversion and hydrogen yield can be obtained in the reforming of methane by incorporation of a hydrogen-selective membrane into a conventional reactor, because of a shift of equilibrium caused by removing hydrogen through a membrane. At the same time, fuel-cell grade hydrogen can be obtained during a reaction in the tube side of a MR (permeate) due to a hydrogen-selective membrane used in a MR without further separation and purification steps, while all other products except hydrogen can be obtained in a shell side of a MR (retentate). Previously, a MR equipped with a hydrogen-selective membrane was applied to various reforming reactions that produce hydrogen such as methane dry reforming ($CH_4+CO_2=2H_2+2CO$) [2,3], methane steam reforming ($CH_4+H_2O=3H_2+CO$) [4-7], methanol steam reforming ($CH_3OH+H_2O=3H_2+CO_2$) [8-10], and ethanol steam reforming ($C_2H_5OH+3H_2O=6H_2+2CO_2$) [11-14] and enhanced reactant conversion and hydro-

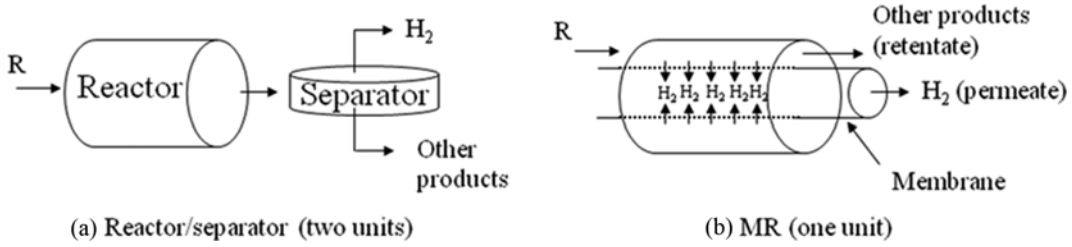

Fig. 1. Comparison between (a) a reactor/separator and (b) a MR.

†To whom correspondence should be addressed.
E-mail: hklim@cu.ac.kr

gen yield in a MR compared to a conventional packed-bed reactor (PBR) without a membrane were reported. Even though the better performance of MRs than PBRs was reported from various research groups, its commercialization was hindered by some challenging issues such as hydrothermal stability for silica-based membranes and high cost for palladium-based membranes. At the same time, many efforts are being made to improve hydrothermal stability and to reduce production cost by introducing some materials to pure silica and palladium membranes.

Similarly, many previous studies have reported the performance enhancement in a MR for a water gas shift reaction (WGSR) (Eq. (1)).

$$CO+H_2O \leftrightarrow CO_2+H_2 \qquad \Delta H^{o}_{298\,K}=-41\ kJ\ mol^{-1} \tag{1}$$

Tosti et al. [15] carried out the reaction over a low-temperature shift catalyst, LK-821-2, at 598-603 K in a MR fitted with Pd-Ag metal foils and observed the CO conversion close to 100% that is well above the equilibrium data of about 80%. Basile et al. [16] performed both experimental and simulation studies using two kinetic models (Temkin and Hinshelwood-Langmuir) and one simplified model for a WGSR in a MR fitted with Pd or Pd-Ag membrane, and found that there was a good agreement between experimental and simulation data. Brunetti et al. [17] reported experimental results of a WGSR in a MR using a hydrogen-selective silica membrane at 220-290 °C and 2-6 bar with the best CO conversion of 95% achieved at 280 °C and 4 bar exceeding an equilibrium conversion of a traditional reactor. H_2/CO_2 selectivity of the silica membrane ranged from 35 to 23 with a temperature range of 225 to 291 °C. Brunetti et al. [18] also did a simulation study for a WGSR in a MR fitted with a Pd-alloy membrane using a main parameter, Damköhler's number (*Da*, a ratio of a reaction rate and a reactant feed rate), and introduced a volume and a conversion index as a simple tool to analyze volume reduction or improved conversion shown in a MR. Barbieri et al. [19] performed experimental studies for a WGSR in a MR equipped with a Pd-alloy membrane using a temperature range of 280-320 °C, an operating pressure up to 600 kPa, and a gas hourly space velocity range of 2,000-4,500 h^{-1}. They reported that there was a significant reduction in a required reactor volume for a MR with a new configuration compared to a typical one. Mendes et al. [20] investigated the effect of using a MR for a WGSR to enhance hydrogen production using a $CuO/ZnO/Al_2O_3$ catalyst and a Pd-Ag membrane under various reaction conditions such as a reaction temperature, a feed pressure, and a feed composition and proved the benefit of a MR with 100% CO conversion and an almost complete hydrogen recovery. In addition, Mendes et al. [21] studied a WGSR both numerically and experimentally in a MR fitted with a Pd-Ag membrane with a commercial $CuO/ZnO/Al_2O_3$ catalyst under various reaction conditions and showed that simulation results based on a one-dimensional and isothermal model were in good agreement with experimental results. Zhang et al. [22] reported some experimental results for a WGSR in a MR using a commercial $CuO/ZnO/Al_2O_3$ catalyst and a hydrogen-selective zeolite membrane with H_2/CO_2 selectivity of 42.6 and a hydrogen permeance of 2.82×10^{-7} mol $m^{-2}s^{-1}Pa^{-1}$ and a higher CO conversion than an equilibrium one was obtained in a MR. Cornaglia et al. [23] reported the use of a new $Pt/La_2O_3{\cdot}SiO_2$ catalyst in a Pd-Ag MR for a WGSR under reaction conditions of 673-723 K and 100-800 kPa and observed a CO conversion of 98% and a hydrogen recovery of 90% in a pressure difference of 700 kPa in a MR. Moreover, Cornaglia et al. [24] studied a WGSR using a $Pt/La_2O_3{\cdot}SiO_2$ catalyst in a Pd-Ag MR experimentally and developed a one-dimensional model for simulation studies to obtain good agreement between experimental and theoretical data.

Although many previous studies have shown the benefit of a MR for a WGSR in terms of an increased CO conversion and a high hydrogen recovery, only the effect of reaction conditions such as temperature, pressure, feed flow rate and feed composition on the conversion of CO and a hydrogen recovery in a MR was investigated. The effect of a wide range of two important parameters of membrane, hydrogen permeance and hydrogen selectivity, on the performance in a MR was not analyzed. Therefore, the goal of this research was to investigate the feasibility of performing a WGSR in a MR for enhanced and purified fuel-cell grade hydrogen compared to equilibrium data using numerically simulated results obtained from a one-dimensional reactor model. In addition, the effect of reaction temperature (423-573 K), and most of all, two important parameters of a membrane, representative hydrogen selectivity over other gases such as CO, H_2O, and CO_2 (4.7 to 10^5, representing a Knudsen region and infinite region, respectively) and hydrogen permeance (1×10^{-8} to 1×10^{-7} mol $m^{-2}s^{-1}Pa^{-1}$), on the performance of a MR is discussed extensively in the paper.

RESULTS AND DISCUSSION

Various reaction kinetic models for a WGSR have been reported so far [25-28] and an empirical rate expression reported by Choi and Stenger [29] over a commercial $Cu/ZnO/Al_2O_3$ catalyst (EX-2248, Sud-Chemie) was chosen for this study. The kinetic model is shown in Eq. (2).

$$r_{CO}=2.96\times10^{5}\exp\left(\frac{-47400}{RT}\right)\left(P_{CO}P_{H_2O}-\frac{P_{CO_2}P_{H_2}}{K_e}\right)$$
$$K_e=\exp\left(\frac{4577.8}{T}-4.33\right) \tag{2}$$

Reactor modeling used in a conventional one-dimensional study was employed for this study [21,30] (see Appendix A). The following assumptions were made in the reactor modeling: (a) steady-state operation, (b) negligible heat transfer, and (c) negligible radial concentration gradients. In addition, a constant hydrogen partial pressure along a reactor length was assumed for this study to only focus

Table 1. Reaction conditions and properties of a tubular membrane used in a MR

Reactant	Co_{in} (mol s^{-1})	10^{-6}
	$CO : H_2O : H_2 : CO_2$	1 : 0.9 : 0.8 : 0.3
Reactor	T (K)	423-573
	Catalyst used (g)	2
Tubular membrane	Length (cm)	4
	Tube diameter (cm)	1
	H_2 permeance (mol $m^{-2}s^{-1}Pa^{-1}$)	10^{-8}-10^{-7}
	H_2 selectivity	4.7-10^5

the effect of different hydrogen permeances from different membranes on the permeance of a MR.

Table 1 shows details of reaction conditions and properties of a tubular membrane used in a MR. The membrane conditions were chosen based on a CO feed flow rate of 10^{-6} mol s^{-1} and the permeance of a gas molecule (Q) is a property obtained by the formula, Q=F/AΔp, where Q is the permeance (mol m^{-2} $s^{-1}Pa^{-1}$) of a gas molecule, F is the molar flow rate (mol s^{-1}), A is the membrane area (m^2), and Δp is the pressure difference between the shell and tube sides of a membrane (Pa). The operating pressure is atmospheric pressure and hydrogen flow permeating through the membrane is driven by a partial pressure difference of hydrogen between shell and tube sides. The hydrogen selectivity is the ratio of hydrogen permeance over other gas molecules' permeance, indicating that a higher hydrogen selectivity means higher hydrogen permeance compared to other gas molecules of interest. Various membranes with different hydrogen permeance and selectivity rather than just a single membrane were chosen for this study to investigate the effect of two parameters, hydrogen permeance and selectivity, on a MR more extensively. The composition of a feed stream for WGSR was obtained from average compositions from various coal gasifiers (GE Energy Radiant, Conoco-Phillips E-Gas, KBR Transport Gasifier, and Shell) [31] to closely simulate actual compositions and the molar ratio of $CO:H_2O:H_2:CO_2$ was 1 : 0.9 : 0.8 : 0.3.

Fig. 2 shows CO conversion results obtained from MRs with a different hydrogen selectivity from 4.7 to 10^5 at a temperature range of 423 K-573 K with thermodynamic equilibrium CO conversions presented for comparison. The hydrogen permeance of a membrane used in a MR was 2×10^{-8} mol $m^{-2}s^{-1}Pa^{-1}$. A hydrogen selectivity of 4.7 represents a Knudsen diffusion region where the permeance of a gas molecule is inversely proportional to the square root of its molecular weight and a hydrogen selectivity of 10^5 represents a nearly infinite hydrogen selectivity often found in palladium membranes [32-34]. First, equilibrium CO conversion decreases with increasing temperature consistent with the fact that a WGSR is exothermic. The equilibrium conversion at 423 K is 87.9% and it decreases to 74.3% (~16% decrease) at 573 K. For all MRs studied, higher CO conversion than equilibrium was observed because of the equilibrium shift confirming the benefit of a MR. Furthermore, there was a clear trend of increasing CO conversion with increasing hydrogen selectivity at the same temperature. For example, CO conversion was 78.3% for a membrane with hydrogen selectivity of 4.7, but it increased to 81.1% for a membrane with hydrogen selectivity of 10^5 at 573 K. At 423 K, the CO conversion was 88.5 for a membrane with a hydrogen selectivity of 4.7 and it slightly increased to 89.0% for a membrane with a hydrogen selectivity of 10^5. It is believed that these phenomena happened because more CO remained and reacted in a retentate side due to the high hydrogen selectivity of a membrane. Interestingly, there was only little increase of CO conversion in a MR when the hydrogen selectivity was higher than 100, which suggests that this hydrogen selectivity of 100 can be considered as a criterion for achieving good performance in a MR. Also, even though CO conversion decreased with increasing temperature due to a thermodynamic reason, CO conversion enhancement, defined as Eq. (3), increased with increasing temperature. For example, for a membrane with a hydrogen selectivity of 100, the CO conversion enhancement relative an equilibrium conversion at 423 K was 1.3%, while the one at 573 K was 9.0%. This result suggests that more benefits of a MR can be obtained at a high temperature even with less CO conversion, and a reaction temperature should be chosen carefully depending on individual needs.

$$\text{Conversion enhancement} = \frac{\text{conversion (MR)} - \text{conversion (Equilibri um)}}{\text{conversion (Equilibriu m)}} \times 100 \quad (3)$$

Fig. 3 presents hydrogen flow in a tube side of a membrane (permeate) fitted with a membrane with a different hydrogen selectivity when the hydrogen permeance of a membrane used was 2×10^{-8} mol $m^{-2}s^{-1}Pa^{-1}$. The hydrogen flow in a permeate side has a significant meaning because it shows how much a purified hydrogen can be obtained in a MR during the reaction with no additional

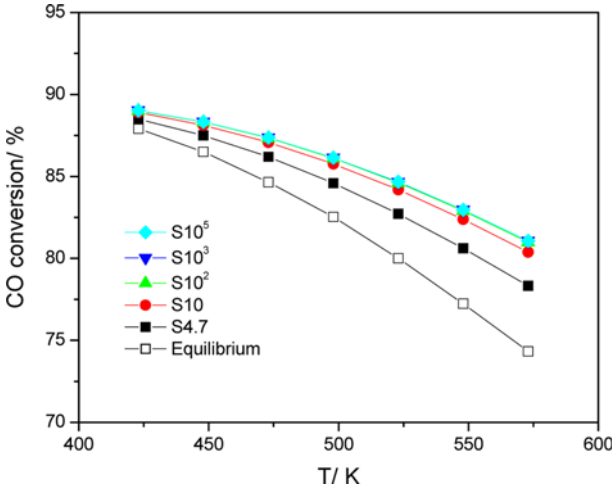

Fig. 2. CO conversion at 423-573 K in a MR with different hydrogen selectivity (S) and a hydrogen permeance of 2×10^{-8} mol $m^{-2}s^{-1}Pa^{-1}$.

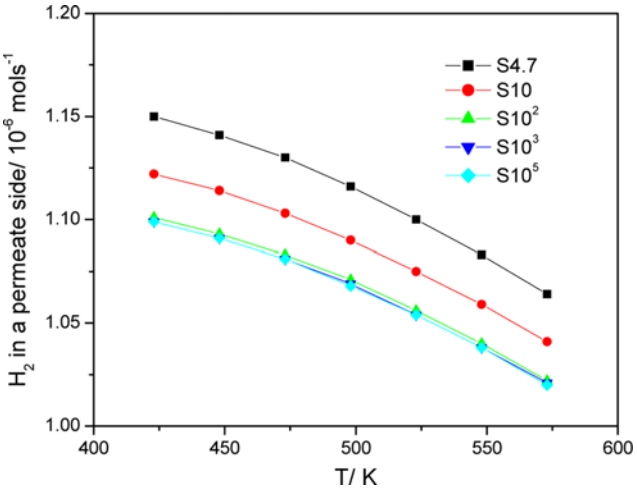

Fig. 3. H_2 flow through a membrane (permeate) at 423-573 K in a MR with a different hydrogen selectivity (S) and a hydrogen permeance of 2×10^{-8} mol $m^{-2}s^{-1}Pa^{-1}$.

Table 2. Effect of hydrogen selectivity on H_2 flow and H_2 purity in a MR

T/K	H_2 selectivity	10	10^2	10^3	10^5
423	H_2 flow decrease/%	2.4	4.3	4.4	4.4
	H_2 purity increase/%	12.1	24.5	25.9	26.1
498	H_2 flow decrease/%	2.3	4.0	4.2	4.3
	H_2 purity increase/%	13.3	26.5	28.0	28.2
573	H_2 flow decrease/%	2.2	3.9	4.0	4.1
	H_2 purity increase/%	15.4	29.9	31.6	31.8

units to separate and purify hydrogen attached. Overall, hydrogen flow in the permeate side decreased as temperature increased because of thermodynamics, and this trend held for all membranes used. Interestingly, for the same temperature, hydrogen flow in the permeate side decreased as hydrogen selectivity increased indicating, that a hydrogen perm-selective membrane was not favorable for higher hydrogen flow. For example, respective hydrogen flows in the permeate side were 1.15×10^{-6} and 1.10×10^{-6} $mols^{-1}$ for membranes with a hydrogen selectivity of 4.7 and 10^5. More quantitative analysis for the phenomena is presented in Table 2 with a hydrogen flow and hydrogen purity in the permeate side. H_2 flow decrease and H_2 purity increase were calculated from the difference between a membrane with a hydrogen selectivity of 10, 10^2, 10^3, and 10^5 and a membrane with a hydrogen selectivity of 4.7. Compared to H_2 flow and purity for the membrane with a hydrogen selectivity of 4.7, there was a significant increase in a hydrogen purity for a membrane with a higher selectivity of 10-10^5 (up to 31.8%) with only a slight decrease in a hydrogen flow (up to 4.4%). The actual concentration of hydrogen in the permeate side was about 75% for a hydrogen selectivity of the Knudsen region, and it gradually increased to about 99.9%, feasible for a fuel-cell grade hydrogen, for a hydrogen selectivity over 10^3. Therefore, it is a better choice to use a membrane with a higher hydrogen selectivity at the expense of a hydrogen flow when high purity hydrogen is needed.

Fig. 4 shows CO concentration in purified hydrogen (permeate) at different temperature and hydrogen selectivity when hydrogen permeance was 2×10^{-8} mol $m^{-2}s^{-1}Pa^{-1}$. The CO concentration increased with increasing temperature because less CO reacted at high temperature, and this is consistent with a thermodynamic expectation. In an equilibrium condition, the range of a calculated CO concentration in a product stream was from 403 to 815 ppm from 423 to 573 K, and this CO concentration is too high to be directly fed to fuel cells. Normally, fuel-cell grade hydrogen is defined as purified hydrogen with a CO concentration below 50 ppm [29]. CO concentration in the permeate side was higher than 100 for a MR fitted with a membrane with hydrogen selectivity of 4.7 ad 10. However, the CO concentration in the MR started to decrease with increasing hydrogen selectivity, and it was less than 50 ppm for all temperatures studied when a membrane with a hydrogen selectivity higher than 100 was used. Therefore, a membrane with a hydrogen selectivity of more than 100 should be used to obtain a fuel-cell grade hydrogen with a CO concentration of less than 50 ppm. Moreover, this proves one advantage of a MR that a purified fuel-cell grade hydrogen can be obtained during the reaction without an additional separation unit.

Fig. 5 presents the effect of hydrogen permeance on the CO conversion enhancement at 473, 523 and 573 K in a MR when a membrane with hydrogen selectivity of 100 was used. The hydrogen permeance ranged from 1×10^{-8} to 1×10^{-7} mol $m^{-2}s^{-1}Pa^{-1}$. It also shows the percentage of hydrogen permeating through a membrane (permeate) in total hydrogen produced (retentate+permeate) with different hydrogen permeance and temperature. CO conversion enhancement increased steadily with hydrogen permeance. It increased from 1.5 to 6.0% at 473 K and from 4.5 to 19.5% at 573 K when hydrogen permeance increased from 1×10^{-8} to 1×10^{-7} mol $m^{-2}s^{-1}Pa^{-1}$. This result strongly supports the need to develop a membrane with a high hydrogen permeance to take full advantage of a MR. However, it reached a plateau when the hydrogen permeance was about 8×10^{-8} mol $m^{-2}s^{-1}Pa^{-1}$, and it is surmised that this happened because the partial pressure difference between retentate and permeate sides,

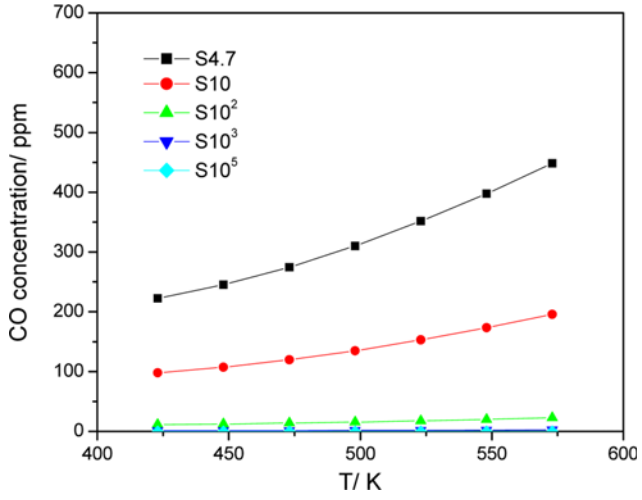

Fig. 4. CO concentration in a purified hydrogen in a MR (permeate) with a different hydrogen selectivity (S) and a hydrogen permeance of 2×10^{-8} mol $m^{-2}s^{-1}Pa^{-1}$.

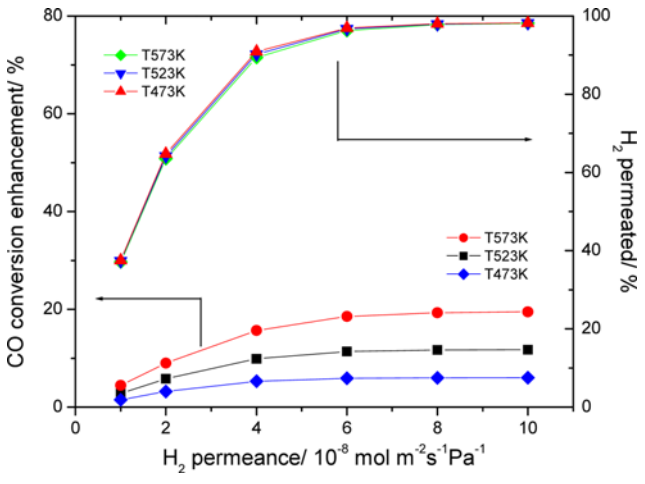

Fig. 5. Effect of H_2 permeance on CO conversion enhancement and the percentage of H_2 in a permeate in a MR with a hydrogen selectivity of 100 at 473, 523, and 573 K.

which is thought a driving force for a hydrogen permeation, started to decrease as a hydrogen permeance increased. In addition, there was a good correlation between CO conversion enhancement and a percentage of hydrogen permeated through the membrane. In other words, a higher hydrogen permeance induced a higher percentage of hydrogen permeating through a membrane, causing more driving force between retentate and permeate sides, and this led to CO conversion enhancement by an equilibrium shift. Consequently, this result also provides a guideline for a minimum hydrogen permeance of 8×10^{-8} mol $m^{-2}s^{-1}Pa^{-1}$ to fully utilize the benefits of a MR for the conditions studied here. This calculated hydrogen permeance is easily obtained from various membranes reported so far, such as silica- and palladium-based membranes; however, it is very challenging to produce hydrothermally stable silica or low-cost palladium membranes as noted before. Therefore, future research directions should be focused on fabricating hydrogen-selective membranes with good hydrothermal stability and low manufacturing cost by incorporating some materials into pure silica or palladium membranes.

Fig. 6 shows the effect of hydrogen permeance on the percentage of hydrogen permeated through a membrane described previously and CO_2 concentration in the retentate side at 473, 523, and 573 K in a MR with a hydrogen selectivity of 100. For temperatures studied, there was little difference for H_2 permeated through a membrane, while there was a slight difference for CO_2 concentration in the retentate side. A higher CO_2 concentration in the retentate side was observed for a lower temperature possible due to more CO_2 production caused by an exothermic WGSR, and the difference became smaller with increased H_2 permeance. As hydrogen permeance increased, both the percentage of hydrogen permeated and CO_2 concentration in the retentate side increased. The percentage of hydrogen permeated increased from 38 to 98% and the CO_2 concentration in the retentate side also increased from 49 to 90% as hydrogen permeance increased from 1×10^{-8} to 1×10^{-7} mol $m^{-2}s^{-1}Pa^{-1}$. In particular, both the percentage of hydrogen permeated and CO_2 concentration in the retentate side reached a plateau

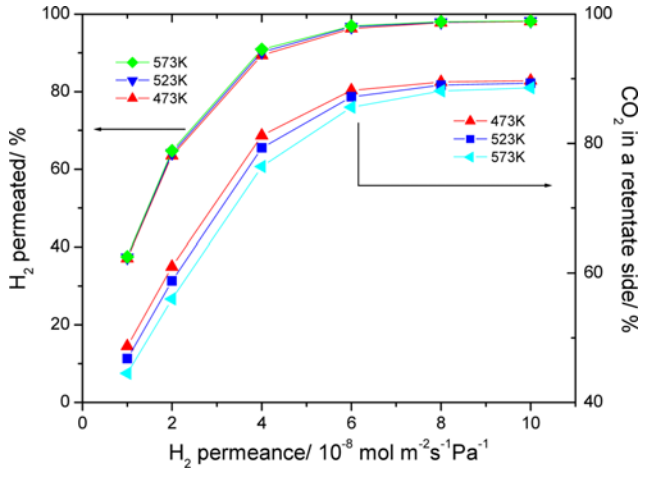

Fig. 6. Effect of H_2 permeance on the percentage of H_2 in a permeate and CO_2 in a retentate at 473 K in a MR with a hydrogen selectivity of 100 at 473, 523, and 573 K.

of 98 and 90%, respectively, and this result opens up the possibility of using a MR as a means to produce a fuel-cell grade hydrogen in the permeate side and concentrated CO_2 in the retentate side at the same time.

CONCLUSIONS

A numerical simulation has been carried out for a WGSR in a membrane reactor (MR) using a feed stream obtained from real coal gasifiers. From 423-573 K, the CO conversion in a MR was higher than equilibrium conversions. Two important parameters of a membrane used in a MR, hydrogen selectivity and hydrogen permeance, were chosen for comprehensive studies and hydrogen selectivity was favorable for CO conversion enhancement and reduced impurities in a purified fuel-cell grade hydrogen, leading to a CO concentration below 50 ppm in a MR with a minimum hydrogen selectivity of 100. Hydrogen permeance was also favorable for CO conversion enhancement in a MR due the increased driving force for hydrogen permeation between the retentate side and permeate side of a MR. In particular, fuel-cell grade hydrogen (CO concentration <50 ppm) was obtained in the permeate side with highly concentrated CO_2 (~90%) in the retentate side at the same time in a MR with a hydrogen permeance higher than 8×10^{-8} mol $m^{-2}s^{-1}Pa^{-1}$ and hydrogen selectivity of 100. These criteria can be easily achieved by various membranes reported so far; however, more hydrothermally stable silica-based membranes and low-cost palladium-based membranes should be developed to open up the possible commercialization of a MR.

ACKNOWLEDGEMENTS

This work was supported by research grants from the Catholic University of Daegu in 2013.

NOMENCLATURE

F_i : molar flow rate of species i on a shell side of MR (retentate) [mol s^{-1}]
F_i^{tube} : molar flow rate of species i on a tube side of MR (permeate) [mol s^{-1}]
W : catalyst weight [g]
r_i : reaction rate equation of reaction i [mol s^{-1} g^{-1}]
r_i^{tube} : permeation rate equation of species i through a membrane [mol s^{-1} g^{-1}]
$K_{H_2}^{tube}$: proportional constant of $r_{H_2}^{tube}$ [mol s^{-1} g^{-1} atm^{-1}]
P_{total} : total pressure on a shell side of MR (retentate) [atm]
$\sum F_i$: total molar flow rate on a shell side of MR (retentate) [mol s^{-1}]
P_i : partial pressure of species i on a shell side of MR (retentate) [atm]
P_{total}^{tube} : total pressure on a tube side of MR (permeate) [atm]
$\sum F_i^{tube}$: total molar flow rate on a tube side of MR (permeate) [mol s^{-1}]
P_i^{tube} : partial pressure of species i on a tube side of MR (permeate) [atm]
Q_{H_2} : hydrogen permeance [mol $m^{-2}s^{-1}Pa^{-1}$]

A_c : cross-sectional area of a membrane [m^2]
α_i : hydrogen selectivity of species i
R : gas constant [8.314 J mol^{-1} K^{-1}]
T : reactor temperature [K]
WGSR : water gas shift reaction
MR : membrane reactor
PBR : packed-bed reactor

REFERENCES

1. J. G. Sanchez Marcano and T. T. Tsotsis, *Catalytic membranes and membrane reactors*, WILEY-VCH, Weinheim (2002).
2. D. Lee, P. Hacarlioglu and S. T. Oyama, *Top. Catal.*, **29**, 45 (2004).
3. S. Irusta, J. Munera, C. Carrara, E. A. Lombardo and L. M. Cornaglia, *Appl. Catal. A: Gen.*, **287**, 147 (2005).
4. T. Tsuru, K. Yamaguchi, T. Yoshioka and M. Asaeda, *AIChE J.*, **50**, 2794 (2004).
5. P. Hacarlioglu, Y. Gu and S. T. Oyama, *J. Nat. Gas Chem.*, **15**, 73 (2006).
6. J. Tong and Y. Matsumura, *Appl. Catal. A: Gen.*, **286**, 226 (2005).
7. C. S. Patil, M. van Sint Annaland and J. A. M. Kuipers, *Chem. Eng. Sci.*, **62**, 2989 (2007).
8. E. Kikuchi, S. Kawabe and M. Matsukata, *J. Jpn. Pet. Inst.*, **46**, 93 (2003).
9. D.-W. Lee, S.-E. Nam, B. Sea, S.-K. Ihm and K.-H. Lee, *Catal. Today*, **118**, 198 (2006).
10. A. Basile, F. Gallucci and L. Paturzo, *Catal. Today*, **104**, 244 (2005).
11. H. Lim, Y. Gu and S. T. Oyama, *J. Membr. Sci.*, **351**, 149 (2010).
12. H. Lim, Y. Gu and S. T. Oyama, *J. Membr. Sci.*, **396**, 119 (2012).
13. S. Tosti, A. Basile, F. Borgognoni, V. Capaldo, S. Cordiner, S. Di Cave, F. Gallucci, C. Rizzello, A. Santucci and E. Traversa, *J. Membr. Sci.*, **308**, 250 (2008).
14. S. Tosti, A. Basile, F. Borgognoni, V. Capaldo, S. Cordiner, S. Di Cave, F. Gallucci, C. Rizzello, A. Santucci and E. Traversa, *J. Membr. Sci.*, **308**, 258 (2008).
15. S. Tosti, A. Basile, G. Chiappetta, C. Rizzello and V. Violante, *Chem. Eng. J.*, **93**, 23 (2003).
16. A. Basile, G. Chiappetta, S. Tosti and V. Violante, *Sep. Purif. Technol.*, **25**, 549 (2001).
17. A. Brunetti, G. Barbieri, E. Drioli, K.-H. Lee, B. Sea and D.-W. Lee, *Chem. Eng. Process.*, **46**, 119 (2007).
18. A. Brunetti, A. Caravella, G. Barbieri and E. Drioli, *J. Membr. Sci.*, **306**, 329 (2007).
19. G. Barbieri, A. Brunetti, G. Tricoli and E. Drioli, *J. Power Sources*, **182**, 160 (2008).
20. D. Mendes, V. Chibante, J.-M. Zheng, S. Tosti, F. Borgognoni, A. Mendes and L. M. Madeira, *Int. J. Hydrogen Energy*, **35**, 12596 (2010).
21. D. Mendes, S. Sá, S. Tosti, J. M. Sousa, L. M. Madeira and A. Mendes, *Chem. Eng. Sci.*, **66**, 2356 (2011).
22. Y. Zhang, Z. Wu, Z. Hong, X. Gu and N. Xu, *Chem. Eng. J.*, **197**, 314 (2012).
23. C. A. Cornaglia, S. Tosti, M. Sansovini, J. Munera and E. A. Lombardo, *Appl. Catal. A: Gen.*, **462-463**, 278 (2013).
24. C. A. Cornaglia, M. E. Adrover, J. F. Múnera, M. N. Pedernera, D. O. Borio and E. A. Lombardo, *Int. J. Hydrogen Energy*, **38**, 10485 (2013).
25. C. P. P. Singh and D. N. Saraf, *Ind. Eng. Chem. Proc. Des. Dev.*, **16**(3), 313 (1977).
26. C. V. Ovesen, P. Stoltze, J. K. Norskov and C. T. Campbell, *J. Catal.*, **134**, 445 (1992).
27. J. Sun, J. DesJardins, J. Buglass and K. Liu, *Int. J. Hydrogen Energy*, **30**, 1259 (2005).
28. A. A. Phatak, N. Koryabkina, S. Rai, J. L. Ratts, W. Ruettinger, R. J. Farrauto, G. E. Blau, W. N. Delgass and F. H. Ribeiro, *Catal. Today*, **123**, 224 (2007).
29. Y. Choi and H. G. Stenger, *J. Power Sources*, **124**, 432 (2003).
30. S. T. Oyama and H. Lim, *Chem. Eng. J.*, **151**, 351 (2009).
31. http://www.netl.doe.gov/technologies/ccbtl/refshelf/pubs/Membrane%20test%20protocol%20v10_2008_final10092008.pdf.
32. D. Pizzi, R. Worth, M. G. Baschetti, G. C. Sarti and K. Noda, *J. Membr. Sci.*, **325**, 446 (2008).
33. Z. W. Dunbar and D. Chu, *J. Power Sources*, **217**, 47 (2012).
34. B. Dittmar, A. Behrens, N. Schödel, M. Rüttinger, Th. Franco, G. Straczewski and R. Dittmeyer, *Int. J. Hydrogen Energy*, **38**, 8759 (2013).

APPENDIX A. ONE-DIMENSIONAL REACTOR MODEL

$$\frac{dF_{CO}}{dW} = -r_{CO} - r_{CO}^{tube} \qquad \frac{dF_{H_2}}{dW} = r_{CO} - r_{H_2}^{tube}$$

$$\frac{dF_{H_2O}}{dW} = -r_{CO} - r_{H_2O}^{tube} \qquad \frac{dF_i^{tube}}{dW} = r_i^{tube}$$

$$\frac{dF_{CO_2}}{dW} = r_{CO} - r_{CO_2}^{tube} \qquad P_i = \frac{F_i}{\sum F_i} P_{total}$$

$$P_i^{tube} = \frac{F_i^{tube}}{\sum F_i^{tube}} P_{total}^{tube}$$

$$r_{H_2}^{tube} = K_{H_2}^{tube}(P_{H_2} - P_{H_2}^{tube})$$

$$K_{H_2}^{tube} = \frac{Q_{H_2} A_c}{W}$$

$$r_i^{tube} = \frac{K_{H_2}^{tube}}{\alpha_i}(P_i - P_i^{tube})$$